

COHERENT STRUCTURES OF A NEUTRALLY STRATIFIED URBAN BOUNDARY LAYER USING LARGE-EDDY SIMULATION

Marieta Cristina L. Castillo*, Jin Zhang*, Manabu Kanda*, Marcus O. Letzel**, Atsushi Inagaki*

*Tokyo Institute of Technology

**Leibniz University of Hannover

Abstract

Coherent structures of a near-neutral urban boundary layer, simulated using a Parallelized Large-Eddy Model (PALM) for a coupled surface layer and a convective mixed layer, were statistically quantified to relate ejection/sweep events, low momentum regions and vortices in the log-layer. Two-point correlations and cross-correlations of fluctuation velocity and swirling strength quantified the size and shape of the coherent structures, as well as gave evidence of the low-momentum region being induced by counter-rotating vortex pairs in the horizontal plane of the log-region. The effects of outer layer motion, as distinguished from inner layer motion by spatial filtering, on the coherent structure signatures were investigated.

Key words: coherent structures, inner/outer layer motions, two-point correlation

1. INTRODUCTION

Coherent structures are responsible for vertical turbulent transfers of momentum, heat, and moisture. There are a number of paradigms and structural signatures regarding the formation and interaction of these coherent structures¹. Yet, the most commonly used and visually identifiable of these are: spatially organized ejections (Q2) and sweeps (Q4), low-momentum regions, and vortices. Ejection/sweep events significantly contribute to turbulence production, and are associated with low-momentum regions that are instrumental in momentum exchange. These low momentum regions in turn are induced by vortical structures. The log-layer is where maximum interaction between inner/outer motions occurs since these layers overlap in this region. Inner layer motion is associated with active turbulence, is due to shear stress from the surface, wholly responsible for vertical turbulent transport, and follows similarity laws². Outer layer motion, on the other hand, is related to inactive turbulence associated with the convective motion in the atmospheric boundary layer, do not contribute to local Reynolds stress, nor does it follow any similarity laws. The objective is to statistically analyze the associations among the ejection/sweep events, low-momentum regions, and vertical vortices on a horizontal plane within the log-layer over an urbanized surface.

2. NUMERICAL PROCEDURE

A near-neutral boundary layer consisting of an urban surface layer and a convective mixing layer, was simulated. A domain consisting of a square array of cubic buildings is $64h \times 64h \times 65h$ along the horizontal and vertical directions, where the atmospheric boundary layer height is about $30h$, h being the building height of 40 m, and a grid resolution of 5 m. A 20 -m/s streamwise wind and 0.1 Km/s surface heat flux were simulated for 3 hours, given the following boundary conditions: cyclic along horizontal domains, non-slip for all surfaces, slip for the top boundary. A parallelized Large-Eddy Simulation model (PALM)³ for the urban boundary layer was used to calculate the non-hydrostatic, incompressible Boussinesq-approximated Navier Stokes Equations, using Piacsek-Williams second-order advection scheme and 3rd-order Runge-Kutta time integration scheme. The Fast Fourier transform is the pressure solver for the Poisson equation, while a mask method⁴ was simplified and optimized to explicitly resolve solid obstacles on a rectangular grid.

3. METHODOLOGY

Ejection/sweep events are proportioned using quadrant analysis of the instantaneous horizontal flow field at the log-layer. Their contributions to the Reynolds stress at the log-layer are also computed. Linear stochastic estimation (LSE)^{5,6} is used to visualize coherent structures. LSE was developed to study large-scale structures by locally representing a random velocity field in terms of given local conditions. LSE approximates the conditional average of the flow vectors, and is proportioned by linear coefficients derived from two-point correlations. Two-point correlation statistically describes the turbulent structure by quantifying spatial linear relationships. Outer motions are distinguished from inner motions by spatially filtering the instantaneous fluctuation velocity (u') using an area of $8h \times 8h$, yielding the optimal contribution to Reynolds stress out of all the filtering lengths⁷. Vorticity is represented by $\lambda_{ci}(\omega_z)/|\omega_z|$, which is the swirling strength with the corresponding sign of vertical vorticity^{1,8,9}.

4. RESULTS

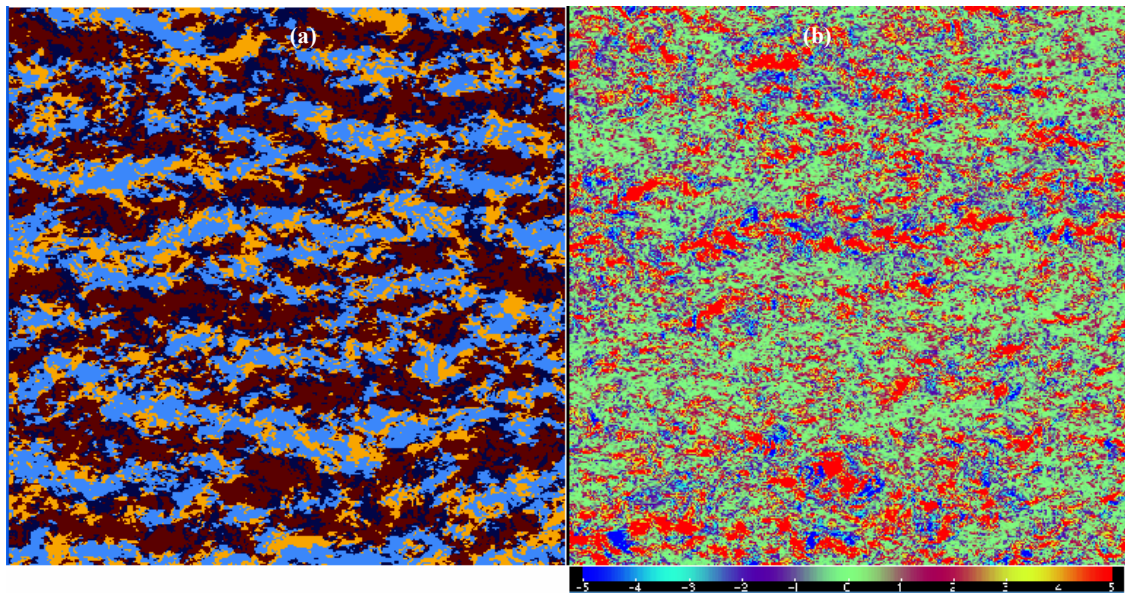


FIGURE 1. Quadrant analysis of filtered flow field: (a) Q1: dark blue, Q2: light blue, Q3: orange, Q4: brown, (b) contribution of local turbulence to Reynolds stress.

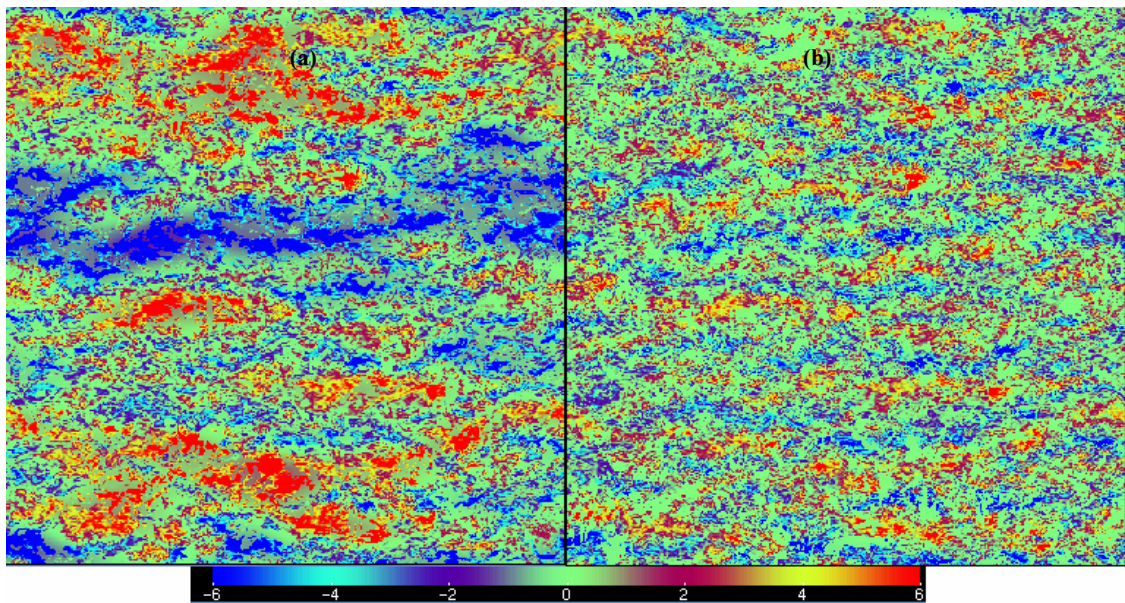


FIGURE 2. Fluctuation velocity field associated with ejection (Q2) and sweep (Q4) events. (a) unfiltered u' (m/s), (b) filtered u'' (m/s).

4.1. Ejection and sweep events

Ejection and sweep events each make up about 30% of the flow field in the log region, as well as dominate in their contribution to Reynolds stress (Fig. 1). By close inspection, the maximum positive contributions are associated with Q2 and Q4 events, as these are responsible for vertical momentum exchange. The flow field associated with these Q2/Q4 events is shown in Fig. 2. Very large structures, which are attributed to outer motion, disappear for the filtered flow field.

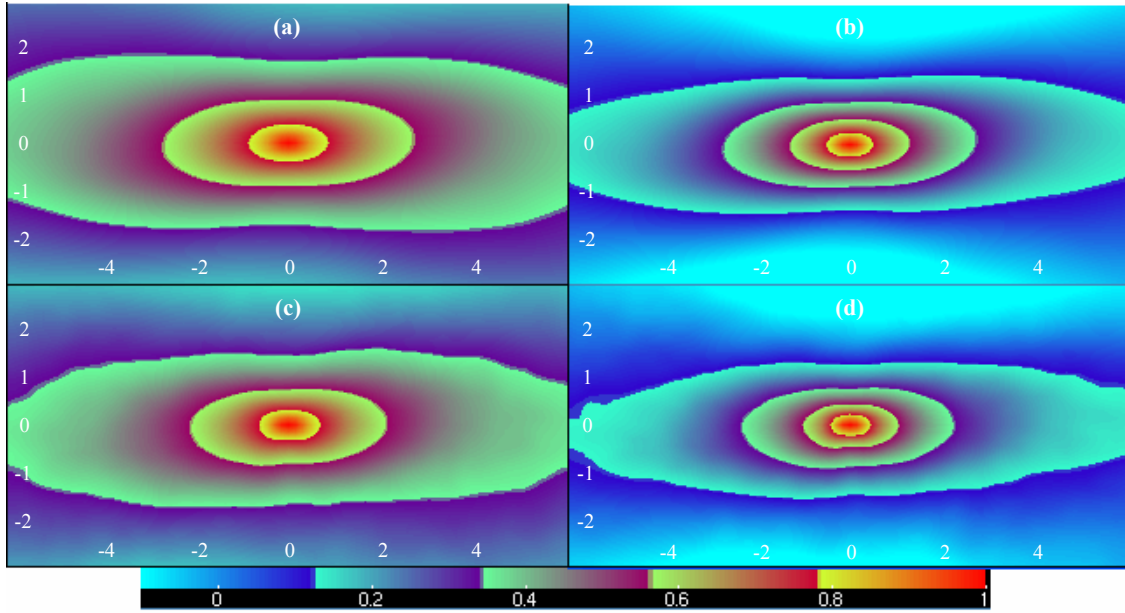


FIGURE 3. Two-point correlations of fluctuation velocity in the log region: (a) unfiltered u' , (b) filtered u'' , (c) conditional average for unfiltered u' , (d) conditional average for filtered u'' . X-axis is streamwise separation $r_x = x/h$, and Y-axis is spanwise separation $r_y = y/h$.

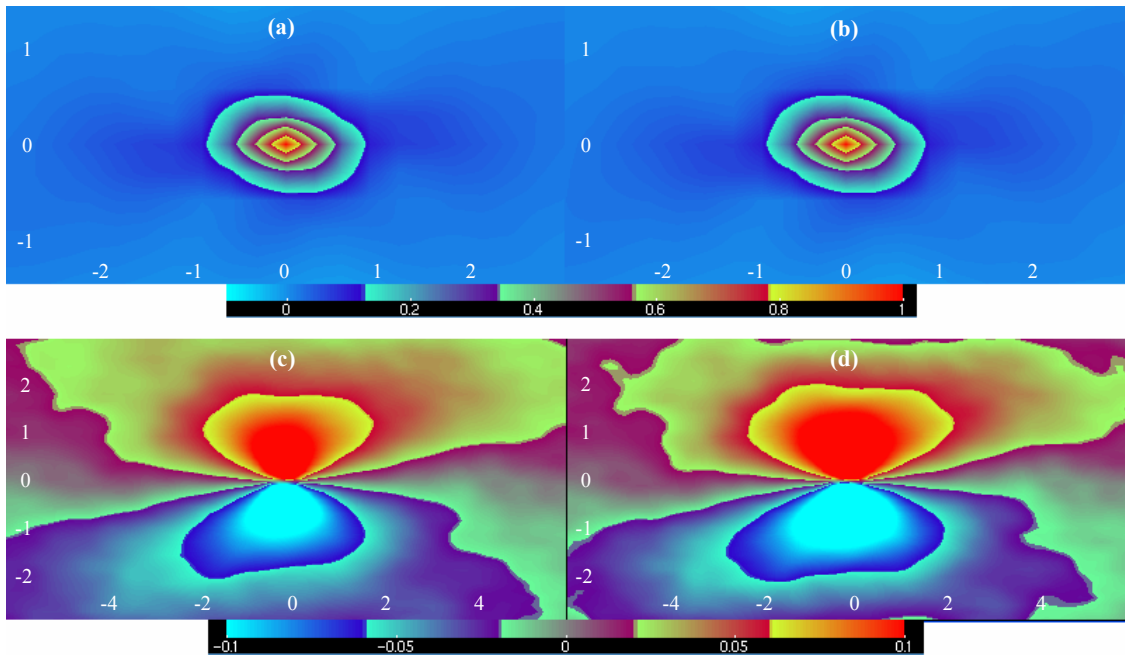


FIGURE 4. Two-point correlations of horizontal velocity fields in the log region: (a) $\lambda_{ci}\omega_z/|\omega_z|$ for unfiltered u' , (b) $\lambda_{ci}\omega_z/|\omega_z|$ for filtered u'' , (c) cross correlation between u' and $\lambda_{ci}\omega_z/|\omega_z|$ for unfiltered flow field, (d) cross correlation between u'' and $\lambda_{ci}\omega_z/|\omega_z|$ for filtered flow field. X-axis is streamwise separation $r_x = x/h$, and Y-axis is spanwise separation $r_y = y/h$.

4.2. Fluctuation velocity field

The conditional average is based on significantly negative fluctuation velocities ($u' < -75\%$ of average u'). In Fig. 3, the two-point correlation contours are elongated along the streamwise, since the vortices in the boundary layer is streamwise-aligned¹⁰. The conditional averages are 20% shorter and 10% thinner than the unconditional correlations. Similarly, the filtered correlations are smaller than the unfiltered ones, yet their overall shape is similarly patterned. This is consistent with the coherent nature of the fluctuation velocity field.

4.3. Swirling strength

The two-point correlation for swirling strength ($\lambda_{ci}\omega_z/|\omega_z|$) is independent of filtering (Fig. 4). It is slightly elongated, which may be due to the presence of hairpin packets^{1,9} and their probable streamwise orientation^{1,10}. The dominance of a single central peak suggests that the vortices travel at consistently the same convection velocity and the frequency of their organization¹⁰. The cross-correlations between fluctuation velocity and swirling strength ($\lambda_{ci}\omega_z/|\omega_z|$) (Fig. 4) are strongest near the streamwise center, positive for $y/h > 0$ and negative for $y/h < 0$. This is consistent with the correlation between a pair of vortices with opposing directions that induce low momentum streaks between them¹⁰. The slight inclination of the cross-correlation contours is attributed to the mutual induction of overlapping vortices of opposing signs, which are responsible in sustaining energy for coherent structures, and that ejection and sweep events occur upstream and downstream of these vortices, respectively⁸. The peaks for the cross-correlations seem to center around the idealized positions of counter-rotating vortex pairs. The location of the peaks (at $y > 0$ and $y < 0$) are more compact for the filtered velocity field. The $u' - \lambda_{ci}\omega_z/|\omega_z|$ -cross-correlations for ejection/sweep events are practically the same as Fig. 4(c) & (d).

4.4. Outer turbulence versus inner turbulence

Ejection/sweep events appear to be affected by outer motion, yet, the proportions of the events, as well as their contribution to the local Reynolds stress, remain unchanged for the filtered flow field. Given the foregoing two-point correlations and cross-correlations, the overall patterns of the coherent structures are generally consistent between the unfiltered and filtered velocity fields. The two-point correlation for the unfiltered u' is about 50% longer and 40% wider than the filtered u' , and are associated with large-scale inactive motions^{1,11}. The fact that the u' -two-point correlation proportions are similar looking and that the λ_{ci} -two-point correlation is independent of filtering, suggest that there is no evidence that the outer motion disturbs the organization of the turbulent flow field and the vertical vorticity in the log region, which have not been previously established⁹. The *dominant, persistent, and well-ordered* vortex organization of outer layer turbulence may contribute to these results^{1,6,9}. The concentration of the cross-correlation peaks towards the idealized position of the counter-rotating vortex pairs for the filtered velocity field illustrates, for inner motion, the robustness of the association between low momentum regions and the counter-rotating vortex pairs.

References

1. Adrian, R. J., Meinhart, C. D., & Tomkins, C. D., 2000: *Vortex organization in the outer region of the turbulent boundary layer*. J. Fluid Mech., 422: 1-54.
2. Townsend, A. A., 1976: *The structure of turbulent shear flow*. Cambridge University Press.
3. Letzel, M. O., Krane, M. & Raasch, S., 2008: *High resolution urban large-eddy simulation studies from street canyon to neighbourhood scale*. Atmos. Env., 42: 8770-8784.
4. Kanda, M., Moriwaki, R. & Kasamatsu, F., 2004: *Large-eddy simulation of turbulent organized structures within and above explicitly resolved cube arrays*. Boundary-Layer Met., 112: 343-368.
5. Adrian, R. J., Moin, P., 1988: *Stochastic estimation of organized turbulent structure: homogeneous shear flow*. J. Fluid Mech., 190: 531-559.
6. Christensen, K. T. & Adrian, R. J., 2001: *Statistical evidence of hairpin vortex packets in wall turbulence*. J. Fluid Mech., 431: 433-443.
7. A. Inagaki, 2008: *Atmospheric turbulence over an array of massive cubes*. Doctoral dissertation, Tokyo Institute of Technology.
8. Jeong, J., Hussain, F., Schoppa, W., & Kim, J., 1997: *Coherent structures near the wall in a turbulent channel flow*. J. Fluid Mech., 332: 185-214.
9. Zhou, J., Adrian, R. J., Balachandar, S., & Kendall, T. M., 1999: *Mechanisms for generating coherent packets of hairpin vortices in channel flow*. J. Fluid Mech., 387: 353-396.
10. Tomkins, C. D., & Adrian, R. J., 2003: *Spanwise structure and scale growth in turbulent boundary layers*. J. Fluid Mech., 490: 37-74.
11. I. Marusic, 2001: *On the role of large-scale structures in wall turbulence*. Phys. Fluids, 13: 735-743.